Cellulose Solutions in Water Containing Metal Complexes[†]

Kay Saalwächter and Walther Burchard*

Institute of Macromolecular Chemistry, University of Freiburg,
Stefan Meier-Str. 31, 79104 Freiburg, Germany

Peter Klüfers, G. Kettenbach, and Peter Mayer

Institute of Inorganic Chemistry, University of Munich, Butenandtstr. 5-13 81377 Munich, Germany

Dieter Klemm and Saran Dugarmaa

Institute of Organic Chemistry and Macromolecular Chemistry, University of Jena,
Humboldtstr. 10, 07743 Jena, Germany

ABSTRACT: Aqueous solutions of a number of metal complexes have been found to dissolve cellulose. Recently, a number of new metal complexes have been developed that completely dissolve cellulose by deprotonating and coordinative binding the hydroxyl groups in the C2 and C3 position of the anhydro glucose. A detailed comparative light scattering study is given for cellulose in Schweizer's reagent (cuoxam), Ni-tren, and Cd-tren. Cuoxam is the well-known solution of cupric hydroxide in aqueous ammonia, and the abbreviation tren stands for tris(2-aminoethyl)amine. Cuoxam and Ni-tren are deep blue solvents. The light scattering measurements were carried out with the blue line of an argon ion laser at wavelength $\lambda_0 = 457.9$ nm, and the data from these solvents required an absorption correction according to the Lambert–Beer law. Cd-tren is almost colorless, and the data could be used without correction. Because of traces of colloid particles, possibly originating from the metal hydroxides, a special treatment for optical clarification became necessary. A large number of samples, cotton linters, various pulp celluloses, and bacterial celluloses, were studied. All three solvents exhibited good solution properties, but only Cd-tren was capable of dissolving also the highest degrees of polymerization of cotton linters and bacterial cellulose ($DP_w = 9700$). The limits for the two other solvents were $DP_w < 6300$ for Ni-tren and $DP_w < 5300$ for cuoxam. A fairly high chain stiffness was found with Kuhn segment lengths of $l_K = 15.8 \pm 1.4$ nm for Cd-tren, $l_K = 10.2 \pm 0.8$ nm for Ni-tren, and $l_K = 13.1 \pm 1.2$ nm for cuoxam, corresponding to characteristic ratios of $C_\infty = 24.6$, 15.4, and 19.4, respectively. The problem of preferential adsorption is discussed.

1. Introduction

Cellulose belongs to the oldest macromolecules known to us. Staudinger's[1] pioneering work in the 20th century on macromolecules started with this biopolymer. Still, after more than 70 years the structures of individual cellulose molecules remain not fully elucidated. This lack of knowledge is an effect of poor solubility even in uncommon solvents. To obtain information at least on the molar mass, Staudinger[2] introduced the polymer analogous substitution of the OH groups, which were considered as the origin for strong aggregation, and applied it to cellulose. For two fully substituted derivatives complete dissolution down to the molecular level was indeed obtained. These are cellulose trinitrate and cellulose tricarbanilate which both are soluble in a large number of common organic solvents.

Besides appreciable efforts invested in the chemistry of derivatization, serious problems remained. Preparation of fully substituted derivatives turned out to be difficult, because the cellulose chains are embedded in a partially crystalline structure[3] that cannot easily be broken up. Not fully substituted derivatives, on the other hand, were found to be strongly aggregated.[4] The samples appear to possess a special supramolecular structure in solution that is reminiscent of the semicrystalline structure of the parental cellulose. Because of these facts, scientists at no time ceased searching for new solvents that are capable of dissolving cellulose directly and molecularly dispersed.

A first success was reported by Schweizer,[5] who discovered that a solution of cupric hydroxide in aqueous ammonia has the power to dissolve cellulose. This solvent is often called cuoxam. We will use this abbreviation despite some criticisms that has been raised against this nomenclature. Suggestions for the mechanism of dissolution were made later. Accordingly, cuoxam coordinatively binds the deprotonated hydroxyl groups in the C2 and C3 positions of the anhydro glucose units (AGU). The validity of this suggestion was recently proven by systematic studies of crystal structures with oligosaccharides, combined with computer simulations and calculations of complex stability constants.[6,7] Further confirmation was obtained from light scattering measurements.[7,8] Figure 1 shows the structure of the complex bound to the AGU. Cuoxam has some disadvantages which consist of easy degradation of the cellulose chain, a deep blue color that inhibits exact light scattering studies, and a restricted dissolution power that is limited to degrees of polymerization of $DP_w < 5000$. Furthermore, strong association occurs already in moderately concentrated solutions.[9] The reason for the restricted solubility was recently disclosed[6,7] but was not known when Jayme started a systematic search for other metal-based cellulose solvents. In the following a special nomenclature is used, a summary of which is given in the Appendix.

Jayme[10] used ethylenediamine (en) and other polydentate ligands to form complexes with metal ions such as Cu^{2+}, Ni^{2+}, Cd^{2+}, Fe^{2+}, and Co^{2+}. His idea was that
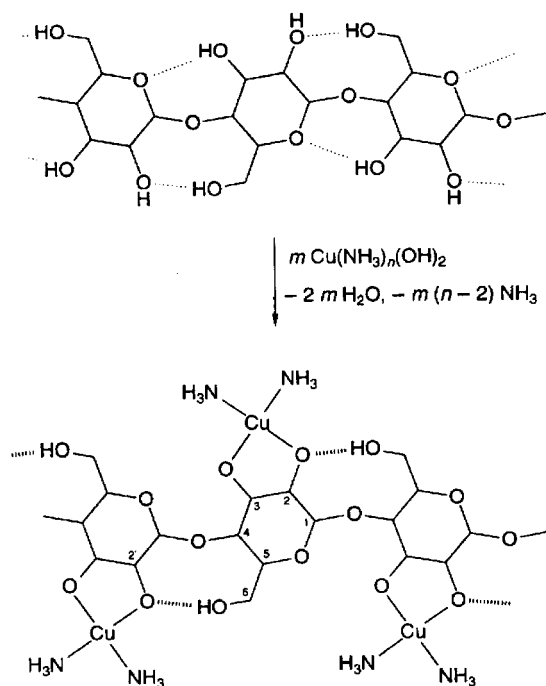
Figure 1. Part of the hydrogen-bonding system in native cellulose and its change after coordinative binding of copper in cuoxam at the deprotonated olate groups in the O2$^-$ and O3$^-$ position of the anhydro glucose unit (AGU). Note: the hydrogen bond between the primary OH group in the C6 position and the ring oxygen of the next AGU is interrupted, but the other hydrogen bond is enhanced. These bonds occur on both sides of the chain and cause an enhanced chain stiffness.[7]

these complexes should have a similar potential of dissolving cellulose as observed with cuoxam. In fact, all these reagents gave clear solutions indicating full solubility of the cellulose. The mechanism of dissolution, however, remained unclear. This question is presently the subject of research in inorganic chemistry.[11] The results of the present investigation are based on exceptional dissolution mechanisms which are rare with synthetic polymers in common organic solvents. The mechanism appears applicable to various polysaccharides but also to other polar polymers. Therefore, the dissolution mechanism may be displayed here at some length before turning to the report of the solution properties of cellulose in three metal-based solvents.

2. Dissolution Mechanism of Metal-Based Solvents

Dissolution of cellulose by nonderivatizing solvents was recognized as being possible by two different mechanisms. In both cases the highly organized hydrogen-bonding system, which surrounds the cellulose chain in the fibrils, has to be broken up. The following consideration may for simplicity be confined to the *intra*chain hydrogen bonds which are effective between the primary OH group in the C6 position of an AGU and the OH group in the C2 position of the neighbored AGU. A second bond is formed on the other side of the stretched chain between the OH group in the C3 position of an AGU and the oxygen of the ring from the neighbored AGU.[12] The hydrogen-bonding system is partially broken when deprotonating both OH groups in the C2 and C3 position.

However, the mere removal of protons by strong alkoxy acceptors is not sufficient to produce solubility

because the cations, associated with anionic alkoxide, undergo Coulomb interactions with the deprotonated anion groups of different chains. Strongly associated ion pairs cause cross-linking and insolubility.[11a] Undesired cross-linking can be prevented by creating solvation separated ion pairs, and this can be achieved sterically by bulky cations, as for instance benzyltrimethylammonium hydroxide (Triton B) or tetraalkylammonia hydroxides. In these cases the cations are not fixed to a special position of the chain, and solubility is induced by common solvation procedures.

The other possibility consists of a strong coordinative binding of the cations where the two deprotonated OH groups in the C2 and C3 position may act as a chelating ligand. This second mechanism is realized with cuoxam, as demonstrated by Figure 1.[7] The two NH$_3$ groups in this complex can be further replaced by two other deprotonated OH groups from an AGU of another chain which results in cross-linking. This Norman compound[13] is a highly swollen gel and is induced by adding NaOH to the cuoxam solution of cellulose. Which reaction actually is observed depends on the stability constants of the corresponding chelates at different pH. Careful spectroscopic measurements and derivation of stability constants for competing complexes with cuoxam[7,14] showed that the equilibrium is shifted toward the Norman compound when the pH is increased beyond a critical value. It also is formed when at constant pH the concentration of cellulose is increased. This competition between two complexes explains the limited concentration range of solubility. It also explains the limiting degree of polymerization that can be dissolved, because long chains can fold back and *intra*molecular cross-linking can take place.[8]

In Cu-en [(NH$_2$−CH$_2$−CH$_2$−NH$_2$)Cu(OH)$_2$] the ammonia groups in cuoxam are replaced by ethylenediamine (en)[15] which causes deprotonation, but coordinative binding to the anionic oxygens in the C2 and C3 position of the glucose ring does not take place. The solvation power is probably solely based on Coulombic interactions of the charged glucose ring combined with a chain separating power of the cations.

This is not true for all ethylenediamine forming complex cations. An exceptional case is observed with the yellow palladium-based solvent Pd-en, an aqueous solution of [(en)Pd(OH)$_2$] that undergoes stable planar coordinative binding with the deprotonated diolate groups of the AGU in cellulose, in a manner that may justify denoting it as a derivatizing solvent. This fact was proven by complexes with oligosaccharides which formed well-defined crystal structures.[7,16] Moreover, there is ^{13}C NMR evidence of virtually complete coordination to cellulose. Good solution behavior of this complex with cellulose was recently demonstrated by Ballauff[17] with light scattering measurements from three samples.

In the search for other metal-based solvents for cellulose that are less expensive than Pd-en, the Ni^{2+} cation appears as a suitable alternative to Cu^{2+}. However, there are some problems regarding coordination equilibria in the case of nickel. Ni^{II} central atoms are coordinated strictly octahedrally to aminine and alkoxo/hydroxo-type ligands, whereas square-planar configurations are favored with copper. Cellulose or low molecular weight diols may thus form coordination compounds of the general formula [(en)$_2$Ni(LH$_{-2}$)] (L = diol) when ethylenedimamine is used to provide the proper number
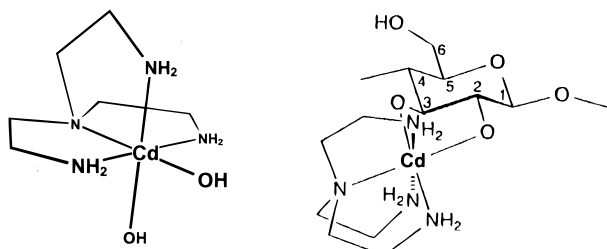
Figure 2. Chemical structure of the Cd-tren(OH)₂ complex and its coordinative binding to the AGU in cellulose.[11] [tren = N(−CH₂−CH₂−NH₂)₃].

of ligands to achieve the octahedral coordination of Ni[II]. However, despite the particularly high stability of analogous [(en)(Cu(LH₋₂)] species,[7] coordination equilibria in en/Ni/diol systems do not favor a species of this kind. Instead, the hypothetical coordination equilibrium

$$3\text{``}[(en)_2Ni(LH_{-2})]\text{''} \leftrightarrow$$
$$2[Ni(en)_3]^{2+} + Ni(OH)_2 + 3L + 4OH^-$$
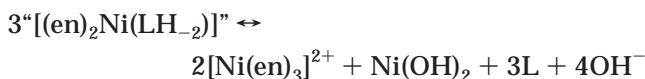
is shifted to the right in the case of ethylenediamine as nitrogen ligand. The formation of a NiN₆-type complex and precipitation of Ni(OH)₂ can be prevented by using a tetradentate chelate ligand as for instance tris(2-aminoethyl)amine (tren).[11a] The corresponding complex leaves two cis-configurated positions at the Ni octahedron free for coordinative binding of the two diolate moieties of the AGU in cellulose. The Ni-tren complex has another advantage of possessing a bulky, rather inert back, thus supporting chain separation by steric interaction. A very similar complex structure is obtained with Cd²⁺ (Cd-tren), which has only a weak yellow color in contrast to Ni-tren which is deep blue. The two metal complexes of Ni-tren and Cd-tren, [Ni(tren)(OH)₂] and [Cd(tren)(OH)₂], turned out to be efficient in dissolving cellulose down to the molecular level. Figure 2 shows the structure of the free complex and in its coordinatively bound state.

In the following we examine the solution properties of cellulose in these two new metal-based solvents and compare these with the corresponding properties in cuoxam. As already mentioned, the study was based on a rigorous investigation of the coordinatively bound structures which were first obtained from crystal structures with suitable oligosaccharides in these solvents. In a further step this knowledge was tentatively generalized by assuming that similar mechanisms may be effective also with the AGU in cellulose.[11] The validity of such considerations was first shown with cellulose in cuoxam[7,8] and led to a sensible explanation of the observed chain stiffness in this solvent.[7] We were interested in learning whether coordinative binding of a metal complex to chains would significantly change common solution properties of polymers. We report light scattering results on molar mass M_w, radius of gyration R_g, second virial coefficient A_2, and Kuhn segment length l_K which describes chain stiffness. In addition, viscosity measurements were performed, and the molar mass dependencies of R_g, R_h, A_2, and the intrinsic viscosity $[\eta]$ were examined. The results from the three solvents Ni-tren, Cd-tren, and cuoxam are compared.

3. General Remarks on Problems with Metal Complexing Solvents

Characterization of linear polymers in organic solvents has become routine work in polymer analysis.

Experimental techniques and methods of data interpretation are well developed. A very different situation is encountered, however, with biopolymers, notably with polysaccharides. The many hydroxyl groups on the chains are capable of uncontrolled hydrogen bonding which often leads to strong association and formation of complex structures. These facts make it necessary to use uncommon solvents. Application of the metal-based solvents impose unanticipated problems. The solvents are often deeply colored, and reliable molar mass determination by light scattering was for a long time considered as not feasible. Only recently reasonable results were obtained for cellulose in cuoxam after applying an absorption correction.[8,9] Nonetheless, reproducible and correct results of the molar mass remain difficult to attain. This has the following reason.

As is well-known, the molar mass of a polymer can be obtained by extrapolating the static light scattering data to zero scattering angle (forward scattering) according to the equation

$$\left[\frac{R_{\theta=0}}{c}\right]_{c \to 0} = KM_w \qquad (1)$$

in which K is an optical constant that describes the contrast of the polymer to the solvent. It contains as essential parameter the refractive index increment $\partial n/\partial c$ and is given by the equation

$$K = \frac{16\pi}{\lambda_0^4 N_a} n_0^2 \left(\frac{\partial n}{\partial c}\right)^2 \qquad (2)$$

where λ_0 is the wavelength of the primary beam light, N_a Avogadro's number, and n_0 the refractive index of the solvent. The refractive index increment is commonly measured in special differential refractometers, in which the refractive index of the solution n is directly compared with that of the solvent. Mostly this type of measurement gives the correct result. However, with the metal complexing solvents a yet nonpredictable effect is obtained by this procedure. A nonnegligible amount of the metal complexing agent is found being bound to the cellulose chain and increases the refractive index of the chain. Simultaneously, the refractive index of the surrounding solvent is slightly decreased. Thus, the differential refractometer measures an refractive index increment that can be considerably smaller than is actually effective in light scattering. The problem can be circumvented when an equilibrium dialysis of the solution against the solvent is performed, and the difference in the refractive indices between these two components is measured.[18] Unfortunately, this procedure is not applicable to cellulose solutions because the membranes in dialysis chambers are based on cellulose or cellulose acetate and become destroyed by the solvent.

Another technique would be the laborious determination of preferential adsorption of the metal compound to the chain as described in detail, e.g., by Strazielle[19] in the book of Hugglin[18] on light scattering.[20] This method is involved with large errors but would be still of interest, because it would give us some idea how many metal compounds are bound to the chain. We refrained from this technique mainly because of the sensitivity of the solvents against air. In addition, we wondered whether the coordinative binding can be described by simple adsorption. It appears conceivable that as a consequence of coordination the cellulose
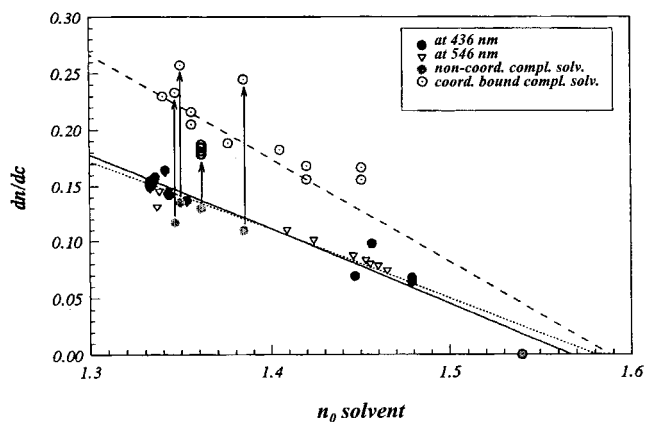
Figure 3. Refractive index increment dn/dc of glucans as a function of the solvent refractive index. Full line: noncoordinative binding at $\lambda_0 = 436$ nm, dotted line at $\lambda_0 = 546$ nm; dashed line coordinative binding, at $\lambda_0 = 436$ nm in metal-based solvents. The arrows indicate the change due to cooperative binding. No difference between the values from different glucans was assumed (see text).

changes its character and thus the refractive index in a nonadditive manner.

Gralén[21] solved the problem of the correct refractive index increment for cuoxam by forming a sharp boundary between solution and solvent in an ultracentrifuge. The difference in the refractive indices was then measured by Schlieren optics. This technique is not particularly accurate because the required sharp boundary is difficult to perform; it soon becomes diffuse due to commencing diffusion. Still our first results[8,9] were obtained with Gralén's value.

Another estimate can be made from the dependence of dn/dc on the solvent refractive index. Figure 3 shows the result for starch in several solvents.[18] The same dependence may be assumed to hold also for cellulose because in both examples the anhydro glucose is a repeating unit. Slight differences are possible but are unlikely, because the same values for dn/dc were found in previous studies for cellulose and amylose tricarbanilates.[22] The refractive index increment for a special solvent now can be found by measuring the refractive index of the solvent and reading off from the graph the corresponding value for dn/dc. However, this value is somewhat too low if applied to the metal complexing solvents, because the refractive index of complexed cellulose is not that for cellulose but is enlarged by the bound metal complex. To find the factor, we prepared the tricarbanilate derivative for a selected number of celluloses and determined the degree of polymerization. The polymer analogous carbanilation is a long known technique,[22] where all the measured chain properties gave no indication for degradation. This value for the degree of polymerization then was compared with that found for the cellulose in the metal complexing solvent using the intrapolated dn/dc. The factors thus evaluated for cuoxam, Ni-tren, and Cd-tren are given in Table 1. The standard deviation for theses data is fairly high and may be estimated to be about ±15%. Most reliable results were obtained with Cd-tren. No absorption correction had to be applied to the almost colorless solvent which improved the accuracy of light scattering data. The uncertainty is highest for Ni-tren because of the deep blue color which required an absorption correction by a factor 3.25 ± 0.25.

Table 1. Refractive Index n_0, Viscosity η_0 (cPa s), and Density d (g/cm³) of Three Metal Complexing Solvents, Refractive Index Increment dn/dc (mL/g) for Cellulose in These Solvents, and Correction Factor f^a

solvent	n_0	dn/dc	η_0	d	correction factor f
Cd-tren	1.347	0.233	1.384	0.9143	1.47 ± 0.23
Ni-tren	1.373	0.199	2.284	1.0891	1.35 ± 0.21
cuoxam	1.375	0.198	2.090	1.1172	1.62 ± 0.16

[a] The measured molar masses have to be multiplied with this correction factor to obtain the same degrees of polymerization as were found for the cellulose tricarbanilate of the same samples. The factor is a measure for the binding strength to the anhydro glucose.

4. Experimental Section

Solvents. *Cuoxam (0.1 M).* A 500 mL aliquot of ice-cooled 25% aqueous ammonia solution was added under argon atmosphere to 5 g (~50 mmol) of Cu(OH)₂ (Aldrich, technical grade). The solution was stirred for about 1 h and then stored at 6 °C in a refrigerator. The solution should be used for measurement within 1 week. Large colloids sensitively disturb light scattering measurements. Precipitated Cu₂O caused no serious problems; these traces could be removed by ultracentrifugation of the solutions immediately before measurement.

Cd-tren (0.8 M). A 102.3 g (0.8 mol) sample of CdO (p.a. >99.5%, Fluka) was dispersed in 140.39 g of freshly distilled tris(2-aminoethyl)amine (tren, pract. >95%, Fluka). The boiling temperature at oil pump vacuum is about 80–100 °C. Distillation did not alter the light yellow color. Mixing should be made gradually under stirring. After 10 min H₂O was added and filled to about 0.9 L. The solution was further stirred at room temperature until a clear solution was obtained. This usually occurred after a few hours, but depending on the quality of the used CdO, sometimes up to 1 week was required. Storing the solutions at 4 °C in the refrigerator accelerated the dissolution process. Remaining traces of CdO were removed by filtration through sintered glass filters. Finally, by adding water the solution was diluted to 1 L. The solution still had a slight yellow color; this gradually disappeared when storing the solution in the refrigerator. After 3 weeks the color was so weak that no absorption correction of the light scattering intensities was needed. Traces of precipitant were removed by filtration immediately before performing light scattering measurements. Cd-tren is highly alkaline, and access of CO₂ should be avoided.

Ni-tren (0.9 M). A 116.3 g (0.4 mol) sample of Ni(NO₃)₂·6H₂O was dissolved in 800 mL of H₂O. A 33.6 g (0.84 mol) sample of NaOH dissolved in 400 mL of H₂O was added under gentle stirring whereupon nickel oxide is formed as a voluminous green precipitant. The precipitant was centrifuged, washed with water, and centrifuged again. The procedure had to be repeated 5–6 times until no nitrate could be detected. The total amount of nickel oxide then was dispersed in a solution of 61.4 g (0.42 mmol) freshly distilled tris(2-aminoethyl)amine (tren, pract., Fluka). A 100 mL aliquot of H₂O were added and stirred for 2 h at 50 °C, avoiding access of oxygen. A deep blue color developed within a short time. The solution was stirred at room temperature for a further 24 h. Excess nickel hydroxide was removed by centrifugation, and H₂O was added to an amount of 500 mL. The deep blue solution is strongly alkaline and absorbs CO₂ but otherwise can be kept in a refrigerator for a long time without loss of quality.

Preparation of Solutions for Light Scattering. A different dissolution and clarification procedure had to be developed for each solvent system.

Cuoxam. Cellulose in cuoxam is sensitive to light and air. To avoid chain degradation during dissolution, each concentration was dissolved separately in brown 25 mL flasks and kept under protecting argon gas atmosphere. All flasks were flushed with argon before filling. The polymer concentration ranged from 0.2 to 5 mg/mL. The solvent was filtered through Anotop ceramic membrane filters of 0.02 μm pore size (Merck) directly into the flasks using a special filter setup that was driven by

a certain pressure of nitrogen gas. The dissolution time was kept as short as possible. In all cases the solutions were prepared in the morning and measured on the same day. Despite all protections, a noticeable degradation of the cellulose chain about 10% was observed by repeated light scattering measurement when keeping a solution overnight. The cotton linters samples became dissolved already after half an hour; for the bacterial cellulose samples and some of the pulp celluloses a somewhat longer time was needed. In all cases a "floating check" was made to prove complete solubility (see section Optical Clarification of Solutions). The solutions then were pipetted into cylindrical light scattering cells, covered by argon gas, and tightly sealed with a stopper that was wrapped by Teflon ribbon and Parafilm.

Ni-tren. For preparation of the solution in Ni-tren no filtration of the solvent was required. Since no degradation of cellulose was found within 1 day, the solutions safely could be prepared the day before measurement. A dilution series of five concentrations in the same range as for the cuoxam solutions was made and transferred into the scattering cells. Further treatment before measurement is described in the next paragraph.

Cd-tren. The Cd-tren solvent contained a considerable amount of large, almost gellike colloidal particles that were visible by eye in the laser light. These particles could not be removed by centrifugation, because of the small difference in density between the highly swollen particles and the solution. Therefore, the solvent was filtered through Anotop ceramic membrane filters of 0.02 μm pore size. The solutions were prepared as described for Ni-tren. The dissolution process of cellulose was appreciably accelerated by cooling the solutions to -15 °C. A 10% degradation of the cellulose was observed when the solutions was stirred overnight. Therefore, the solutions were prepared in the morning and measured the same day.

Optical Clarification of Solutions. The final optical clarification for the light scattering measurements was achieved by ultracentrifugation applying the floating technique of Dandliker.[23] To this end the sealed LS cells were put in the UZ beakers of a swinging bucket rotor that were filled with a concentrated solution of K_2HPO_4. The concentration of the aqueous salt solution was increased until the LS cell started to float. The floated cells were centrifuged at 12 000 rpm. A preparative ultracentrifuge L5-50B (Beckman, USA) was used. In all cases a floating check was made; i.e., the cell was centrifuged for different times, and the solutions were checked whether there was a change in the scattering intensity. If a considerable amount of material was removed by centrifugation, the curves in Zimm plots of the scattering intensities were shifted to larger values.

No change was observed with Ni-tren and Cd-tren; only the colloidal hydroxides were removed. The colloids seriously disturb the angular dependence of the scattered light and cause a strong downturn in the Zimm plot at small angles. This effect disappeared after centrifugation. A different situation was observed with the cuoxam solutions. With freshly prepared solutions the effect of centrifugation was the same as for the two other solvents. No change was observed after centrifugation for 20 and 40 min, respectively. However, when the solution after LS measurements was centrifuged again, the described shift of the curves in the Zimm plot occurred. Figure 4 shows an example. Apparently removed colloidal particles were formed again after a certain time. Possibly these particles adsorb a considerable amount of cellulose, and these aggregates are removed by centrifugation. Because of the low viscosity of cuoxam, solutions could be clarified already after 30–45 min of centrifugation. For Cd-tren and Ni-tren solutions a much longer centrifugation time of about 100 min was required. Figure 5 demonstrates with two examples of Zimm plots the accuracy that was obtained.

Light Scattering Measurements. *Solvent Parameters.* Table 1 gives a list of solvent parameters. The refractive indices and refractive index increments are needed for the calculation of the contrast factors K in eq 2. The refractive index is also required for calculating the light wavelength in
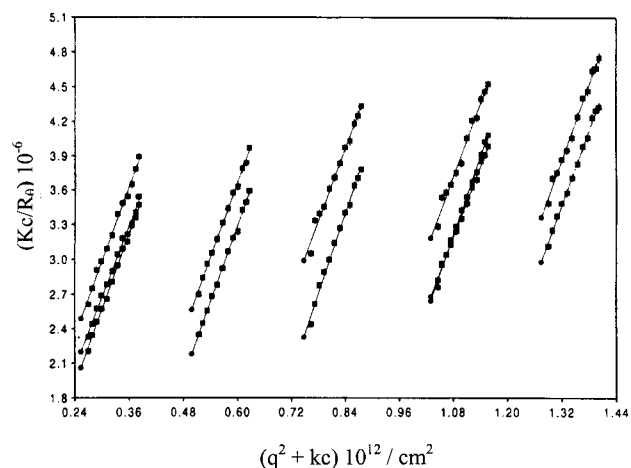
Figure 4. "Floating check". Freshly prepared and immediately after dissolution (within at most 6 h) measured solutions of cellulose in cuoxam show no change in the scattering behavior when centrifuged for 20 and 40 min (the two lower sets of curves). The same solutions centrifuged again 6 h after the performed measurements display a shift to larger values of the reciprocal scattering intensities (upper set of curves). Apparently a certain amount of the cellulose was now removed.
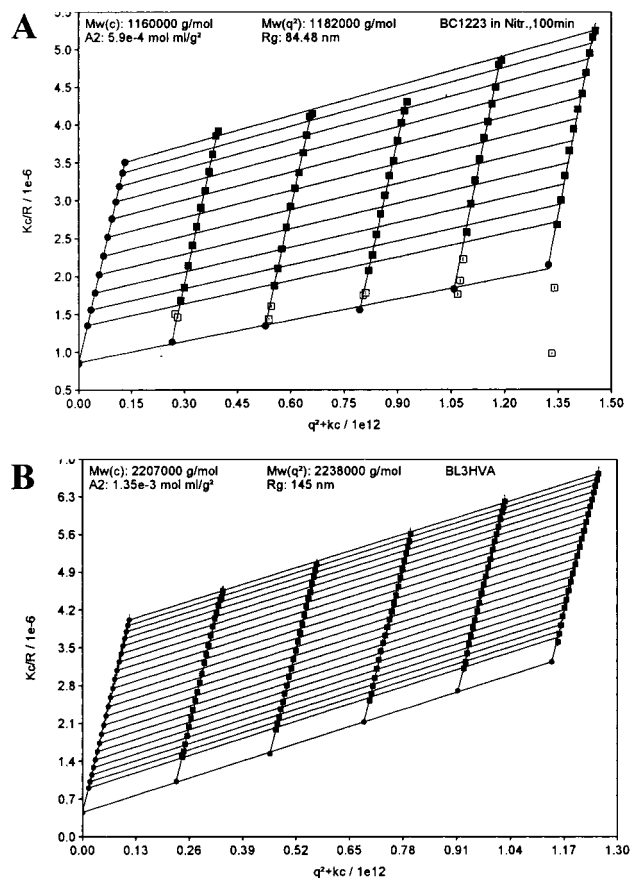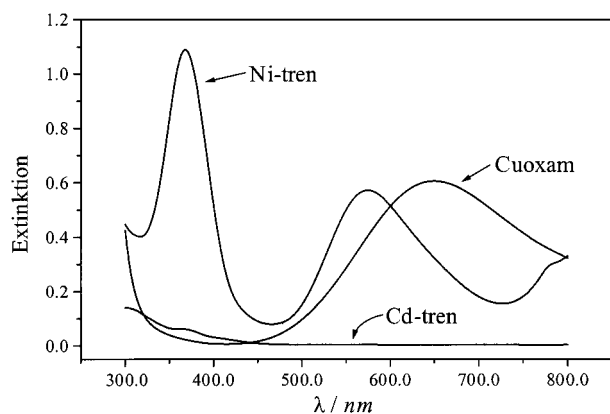

Figure 5. Typical Zimm plots for cellulose: (A) BC 122.3 in Ni-tren, $M_w = 1.18 \times 10^6$ g/mol, $R_g = 84$ nm; (B) Lin3 in Cd-tren, $M_w = 2.24 \times 10^6$ g/mol, $R_g = 145$ nm.

the solvent which is $\lambda = \lambda_0/n_0$. The solvent viscosity enters the Stokes–Einstein relationship

$$R_h = \frac{kT}{6\pi\eta_0 D} \tag{3}$$

according to which the hydrodynamic radius R_h of the macromolecules can be derived from the translational diffusion

Figure 6. Absorption spectra of Ni-tren, cuoxam, and Cd-tren. Light scattering measurements were made at $\lambda_0 = 457.9$ nm for Ni-tren and $\lambda_0 = 488$ nm for cuoxam and Cd-tren. The correction factors were $f_e = 3.77$ for Ni-tren and $f_e = 1.47$ for cuoxam, by which the scattering intesity had to be multiplied. No correction was necessary for Cd-tren.

coefficient D_{trans}, which is measured in dynamic LS. As already mentioned, the refractive index increments were obtained from a linear relationship of dn/dc as a function of n_0. Linear regression of literature data gave the relationship (see Figure 3)

$$dn/dc = 1.468 - 0.924n_0 \tag{4}$$

It may be repeated here that no difference in dn/dc was observed for amylose and cellulose tricaranilates. We see no reason to expect differences also for amylose and cellulose in the metal-based solvents.[9] Furthermore, eq 4 does not contain the influence of the coordinative binding of the metal compounds. The viscosity of the solvent was obtained by measuring the kinematic viscosity in an Oswald viscometer that was corrected by the solvent density for the correct viscosity.

Absorption Correction. In colored solvents the scattering intensity is often remarkably reduced. This reduction of intensity could be accounted for by measuring the extinction E of the solvent and applying Lambert–Beer's law in which the actual diameter of the LS cell ($d = 0.8$ cm) was inserted. Figure 6 shows the absorption spectra for the three metal complexing solvents. The selected blue line of the argon laser had the wavelength $\lambda_0 = 457.9$ nm, which is close to the minima for cuoxam ($\lambda_{0\,min} = 410$ nm) and Ni-tren ($\lambda_{0\,min} = 465$ nm) absorption curves. For the Cd-tren solutions the stronger line of $\lambda_0 = 488$ nm was chosen. The correction factors were $f \approx 1.47$ for cuoxam and $f \approx 3.77$ for Ni-tren. No correction was necessary for Cd-tren.

Static Light Scattering. Measurements in Cd-tren were made with a modified SOFICA instrument (design: G. Baur Apparatebau, Hausach, Germany). The instrument is fully computer driven and is based on a new concept for the detection electronics with improved accuracy. The blue line ($\lambda_0 = 488$ nm) of a 10 mW argon laser (Uniphase, Eching, Germany) was used, and the angular dependence of the scattering intensity was measured in steps of 5° in a range from 30° to 145°. On-line software programs for Zimm, Berry, and Guinier plots facilitated the evaluation of molar mas M_w, radius of gyration R_g, and second virial coefficient A_2. The static LS measurements in cuoxam and Ni-tren were made with the equipment for dynamic LS as described in the next paragraph. The change of instruments was necessary because the required wavelength of $\lambda_0 = 457.9$ nm could only be chosen with the 3 W argon ion laser (Spectra Physics, Darmstadt, Germany).

Dynamic Light Scattering. An ALV goniometer (ALV-Vertrieb, Langen, Germany) was used that was equipped with a 3 W argon ion laser (Spectra Physics). Time correlation functions were measured with an ALV 5000 correlator covering a time domain from 10^{-6} to 10^4 s in one run. Measurements

were made in steps of 10° in the range from 30° to 140°. Evaluation by cumulant fits was made only for the cuoxam solutions. In Cd-tren and Ni-tren remaining colloid particles disturbed this analysis. In these cases the analysis was made via Kohlrausch–Williams–Watts stretched exponential curves.[24] By this technique the relaxation times for each mode could be determined, and the required first cumulant (that no longer contained the contribution of the solvents colloids) was then reconstructed.

5. Theory

Static and dynamic light scattering measurements are common techniques in polymer science. Therefore, the following relationships are given without special comments. For detailed information textbooks[25–27] may be consulted.

Evaluation of *static* LS data is commonly made on the basis of the Debye equation

$$\frac{Kc}{R_\theta} = \frac{1}{M_w P_z(q)} + 2A_2 c \tag{5}$$

The contrast factor was already given by eq 2, and c is the weight concentration in g/mL. $P_z(q)$ is the particle scattering factor that is sensitive to the structure of the molecules in solution. For small values of qR_g it is given by the following equation

$$\frac{1}{P_z(q)} = 1 + \frac{1}{3}q^2 R_g{}^2 + \dots \tag{6}$$

with

$$q = \left(\frac{4\pi n_0}{\lambda_0}\right) \sin\left(\frac{\theta}{2}\right) \tag{7}$$

where θ is the scattering angle. All other quantities have the common meaning. The subscript z denotes the z-average. Thus, from the intercept at $c = 0$ and $q = 0$ the molar mass M_w is obtained, and from the initial slopes of the limiting curves $c = 0$ and $q = 0$ the radius of gyration R_g and the second virial coefficient A_2, respectively, are found.

In *dynamic* LS a normalized intensity–time correlation function (TCF)

$$g_2(t,q) \equiv \frac{\langle i(0,q)\, i(t,q)\rangle}{\langle i(0,q)\rangle^2} \tag{8}$$

is measured, where $i(t)$ is the scattering intensity at a certain delay time from a reference time $t = 0$. In dilute solution this intensity TCF can be expressed in terms of the normalized field TCF using the Siegert[25] relationship

$$g_2(t,q) = 1 + \beta|g_1(t,q)|^2 \tag{9}$$

with a coefficient β that depends on the quality of coherence. For short delay times $g_1(t,q)$ is well approximated by an exponential decay

$$g_1(t,q) \approx \exp(-q^2 D_{app}(q)t) \tag{10}$$

with

$$D_{app}(c,q \rightarrow 0) \equiv D_c \approx D_{trans}(1 + k_D c) \tag{11}$$

where k_D is a coefficient that describes the concentration

Table 2. Origin of Investigated Cellulose Samples[a]

sample	origin of cellulose	DP_η	water content (%)
Lin0	purified cotton linters	800	4.84
Lin1	buckey linters 4403/020	1470	5.00
Lin2	buckey linters 4410/030	2000	5.61
Lin3	buckey linters (Memphis)	7000	1.02
Avicel	microcrystalline cellulose PH-101, Fluka	280	5.06
BC122.2	bacterial cellusoe (laboratory of Jena)		ca. 5
BC122.3	bacterial cellulose (laboratory of Jena)		ca. 5
BC125.1	bacterial cellulose (laboratory of Jena)		ca. 5
BC125.3	bacterial cellulose (laboratory of Jena)		ca. 5
BC125.4	bacterial cellulose (laboratory of Jena)		ca. 5
BC125.5	bacterial cellulose (laboratory of Jena)		ca. 5
BCkr2	bacterial cellulose (laboratory of Jena)		ca. 5
Mcell	pulp cellulose MODO, Rhone-Poulenc Rhodia	570	8.32
Ecell	eucalyptus-pulp cellulose		6.54
Cell1	buckey prehydrolyzed sulfate-pulp cellulose V-60	800	2.34
Cell2	buckey prehydrolyzed sulfate-pulp cellulose V-6	2000	1.25
Cell0	borregarde sulfit-pulp cellulose	800	1.24
RCell1	rayaceta (irradiated pulp cellulose, 100kGy)	350	5.98
RCell2	rayaceta (irradiated pulp cellulose, 60 kGy)	430	5.73
RCell3	rayaceta (irradiated pulp cellulose, 40 kGy)	450	5.76

[a] The DP_η, determined from viscosity in cuen, was provided by the companies. The water content was determined in our laboratory.

Table 3. Molar Masses (in kg/mol) and Corresponding Degrees of Polymerization of Cellulose Determined from Solutions in Cd-tren, Ni-tren, and Cuoxam with the Optical Parameters of Table 1[a]

sample	via CTC		Cd-tren		Ni-tren		cuoxam	
	DP_w	M_w	M_w	DP_w	M_w	DP_w	M_w	DP_w
Lin0	900	145.9	283	1188	274.9	1256	257	978
Lin1			337	1415	300.4	1372	301	1146
Lin2			491	2062	473	2176	514	1957
Lin3			2290	10035	1710	7811	n.s.[b]	n.s.
Avicel			56.0	235	52.6	240	54.3	207
BC122.2	5107	828	1318	5534	1200	5481	1360	5178
BC122.3	6267	1200	1502	6383	1160	5299	1460	5558
BC125.1	5383	872.8	1070	4493	1001	4573	n.s.	n.s.
BC125.3	8111	1320	1690	7091	n.s.	n.s.	n.s.	n.s.
BC125.4	5258[c]	862.6	2371	9956	n.s.	n.s.	n.s.	n.s.
BC125.5	5651	916.2	1361	5715	n.s.	n.s.	n.s.	n.s.
BCkr			807	3386				
Mcel			214	898				
ECel			320	1344	291.7	1333	318	1211
Cel0			420	1763	376.1	1718	398	1515
Cel1			256	1075	252.9	1155	270	1028
Cel2			466	1957	431.7	1972	452	1721
Rcel1			136	571	132.7	606	145	552
Rcel2			178	747	175.1	800	212	807
Rcel3			218	915	193.5	884	235	895

[a] From a linters sample and five bacterial celluloses the cellulose tricabanilate (CTC) derivatives were prepared and measured by LS in dioxan. The corresponding degree of polymerization was determined and the corresponding cellulose molar mass derived. These data served as basis for the determination of the correction factor *f* listed in Table 1; for details see text. [b] n.s. = sample was not completely soluble. [c] This value is evidently too low; it was not included in the calibration.

dependence. A double extrapolation of $D_{app}(c,q)$ has to be performed to get the translational diffusion coefficient required in eq 3 for the derivation of the hydrodynamic radius R_h.

6. Results

Samples. Three cellulose types were characterized by static and dynamic light scattering and by capillary viscometry in the dilute regime. The first group consisted of four native cotton linters samples, $DP_w = 970-9300$, and a highly degraded microcrystalline cellulose (Avicel $DP_w = 280$). The second group contained bacterial celluloses synthesized in Jena by *Acetobacter xylinium*.[25] The degree of polymerization could be varied in a range of $DP_w = 3300-9700$ by changing nutrition conditions. The last group consisted of commercially available pulp celluloses. Details of the cellulose origin are given in Table 2.

The molar masses and degrees of polymerization in the three metal-based solvents are given in Table 3 and are compared with the data of some cellulose tricarbanilates (CTC). The molar masses in the metal-based solvents are in all cases larger than derived from the CTC samples, which reflects the effect of coordinative binding of the complex to the cellulose chain. The ratio of the molar masses gives the correction factors of Table 1. The factors of Table 1 were obtained as follows. We first determined the ratio of molar masses for the five samples measured in Cd-tren. In a second step the average factor between Ni-tren and Cd-tren and between cuoxam and Cd-tren were determined and multiplied by the factor for Cd-tren. All data of the following results refer to molar masses corrected by these factors. The values of the correction factors are all larger than unity and can be considered as a measure of coordinative binding strength.

Table 4. Molar Mass M_w (kg/mol), Radius of Gyration R_g (nm), Hydrodynamic Radius R_h (nm), and Second Virial Coefficient A_2 (mol mL/g^2) of Cellulose in Cd-tren, Ni-tren, and Cuoxam[a]

sample	Cd-tren				Ni-tren				cuoxam			
	M_w	R_g	R_h	$10^4 A_2$	M_w	R_g	R_h	$10^4 A_2$	M_w	R_g	R_h	$10^4 A_2$
Lin0	283	41	23	15.1	275	42	19	11.6	257	41	17	8.5
Lin1	337	48	27	15.5	300	39	15	93	301	43	18	8.9
Lin2	492	54	31	13.4	476	53	19	10.7	514	57	25	11.0
Lin3	2390	134	78	11.6	1711	101	44	6.3				
Avicel	56.0	21	11	16.0	52.6	20	8	13.3	54.3	19	7	13.9
BC122.2	1318	91	66	9.5	1124	84	29	5.9	1360	88	38	7.6
BC122.3	1502	98	68	9.7	1160	85	33	5.9	1462	103	44	9.9
BC125.1	1070	85	54	10.3	1001	76	32	6.0	n.s.	n.s.	n.s.	n.s.
BC125.3	2070	124	66	10.6	n.s.	n.s.	n.s.	n.s.	n.s.	n.s.	n.s.	n.s.
BC125.4	2371	127	70	10.9	n.s.	n.s.	n.s.	n.s.	n.s.	n.s.	n.s.	n.s.
BC125.5	1631	106	58	8.5	n.s.	n.s.	n.s.	n.s.	n.s.	n.s.	n.s.	n.s.
Cel0	421	59	37	12.6	376	55	21	9.5	398	57	23	11.3
Cel1	257	43	24	13.5	253	46	17	12.2	270	39	18	10.0
Cel2	465	60	35	13.8	432	56	21	11.0	452	56	24	8.6
Mcel	213	40	27	10.1								
ECel	320	50		11.1	292	45	18	8.5	318	47	19	13.4
RCel1	136	40	21	15.1								
RCel2	178	42	23	13.2								
RCel3	219	45	28	10.5								

[a] Note: the molar masses were not corrected with the calibration factors *f* as given by Table 1.

Dimensions of Cellulose Chains. Evaluations of static LS intensities were made from common Zimm plots or Berry plots. The corresponding dynamic LS measurements were obtained from dynamic Zimm plots, which are similar to the static Zimm plots but now $D_{app}(q,c)$, instead of Kc/R_θ, is plotted against $q^2 + kc$. As was shown in previous papers,[29] the combination of static with dynamic Zimm plots gives in favorite cases six parameters, which are M_w, R_g, A_2 (static LS), D_{trans} or R_h, a coefficient C, and another coefficient k_D (dynamic LS), where the parameters in the two sets correspond to the intercept, initial slope of the angular dependence, and initial slope in the concentration dependence, respectively. The coefficient k_D was already defined in eq 11; it depends on thermodynamic and hydrodynamic interactions among the particles and is sometime called a *dynamic* virial coefficient. The coefficient C is defined by the following relationship:[27]

$$D_{app}(q,c) = D_c(1 + Cq^2 R_g^2) \quad (12)$$

It contains the influence of the longest internal mode of segmental motion.[30,31]

All molecular parameters depend on the molar mass (see Table 4). Figure 7 shows the result for R_g and R_h in Cd-tren and Ni-tren. The filled symbols refer to native celluloses (cotton linters and bacterial celluloses) and the open symbols to pulp celluloses. The results from the two solvents look very similar to each other, but the ratio of the radius of gyration to the hydrodynamic radius is larger in Ni-tren than in Cd-tren. Furthermore, the data from pulp celluloses are in every case larger than those from native celluloses. This may have two reasons. It can mean either that the extraction procedure from wood caused a slight but significant chemical modification, for instance, by introducing electrolytic charges to the chain, or that the accompanying hemicelluloses were not sufficiently well removed. In both cases a chain stretching is to be expected via Coulomb repulsion in polyelectrolytes or via side-by-side adsorption of hemicellulose chains.

The results of R_g from the cuoxam solutions are plotted in Figure 8 where the data from freshly prepared samples (filled symbols) are compared with those previ-
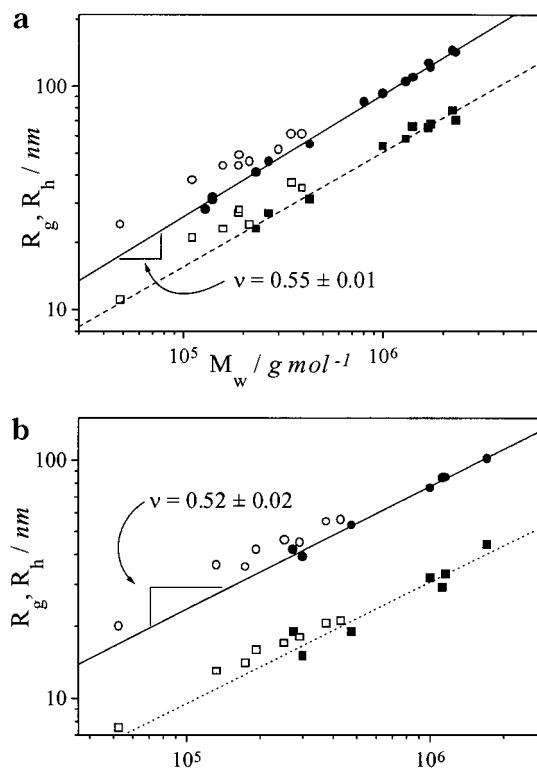
Figure 7. Molar mass dependencies of the radius of gyration R_g (upper curves) and hydrodynamic radius R_h (lower curves) for cellulose (a) in Cd-tren and (b) in Ni-tren. Filled symbols: native and bacterial celluloses; open symbols: pulp celluloses of different origin.

ously published by Seger et al.[8,32] Searching for reasons of the deviations, we noticed that in the previous study solutions were prepared the evening before measurement. Repeat of this procedure in the present study disclosed that aging occurred. New solvent aggregates were formed, and these were strongly coupled to the cellulose chain. This conclusion was drawn from the fact that an appreciable amount of cellulose was now removed by centrifugation which did not occur with freshly prepared solutions and immediate measurement after dissolution. However, the preparation of cellulose
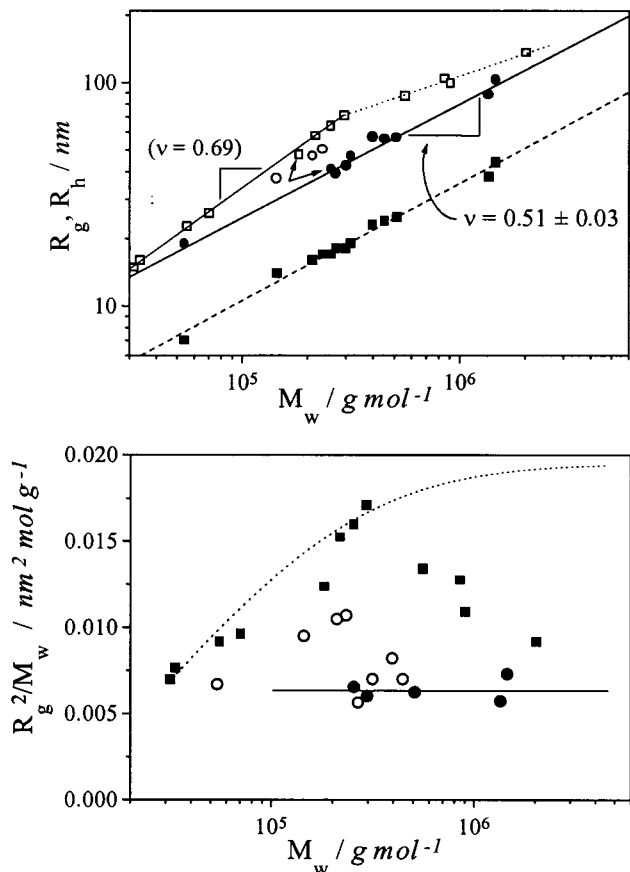
Figure 8. Top: R_g (filled circles) and R_h (filled squares) as a function of M_w for cellulose in cuoxam (this sudy). No differentiation of the various cellulose types was made. The open squares correspond to earlier measurements[8] where the solutions were prepared 12 h before measurement. Because of aggregation the concentration was decreased and resulted in apparent molar masses that are too large (see text). Bottom: ratio R_g^2/M_w as a function of M_w. Filled symbols correspond to native and open symbols to pulp celluloses.

solutions in cuoxam is delicate, and slight changes in the procedure may result in different properties.

The curves in Figures 7 and 8 can be well described by power laws, for instance

$$R_g = K_{R_g} M_w^{\nu} g \tag{13}$$

and a similar relationship for R_h. The exponents are given in Table 5 together with the other exponents for the second virial coefficient and the intrinsic viscosity.

Intrinsic Viscosity. The intrinsic viscosity is usually determined by linear extrapolation of the reduced viscosity against zero concentration according to the relationship

$$\frac{\eta_{sp}}{c} = [\eta](1 + k_H[\eta]c + ...) \tag{14}$$

neglecting higher terms in concentration, where k_H is Huggins' constant. The high molar mass celluloses, however, exhibited a significant quadratic term. Such behavior seems to be typical for cellulose derivatives and was already observed by Schulz[33] many years ago. He suggested a plot of η_{sp}/c against η_{sp}. This plot, known as the Schulz–Blaschke plot,[33] gave a linearization of the concentration dependence. Figure 9 shows that such a linearization was also obtained with the present

Table 5. Experimental Molecular Parameters Compared with Theoretical Prediction[a]

	Cd-tren	Ni-tren	cuoxam
ν_{exp}	0.55 ± 0.01	0.52 ± 0.02	0.51 ± 0.03
K_{R_g} (nm mol$^\nu$/g$^\nu$)	0.047 ± 0.007	0.062 ± 0.019	0.071 ± 0.030
$\rho = R_g/R_h$	1.84 ± 0.14	2.59 ± 0.19	2.51 ± 0.24
a_η	0.72 ± 0.03		0.81 ± 0.03
$\nu_{scal,\eta}$	0.57 ± 0.01		0.61 ± 0.02
K_η (mL/g)	2.64 ± 0.56		0.77 ± 0.03
A_{A_2}	-0.12 ± 0.03	-0.28 ± 0.04	-0.09 ± 0.06
ν_{scal,A_2}	0.63 ± 0.01	0.57 ± 0.01	0.64 ± 0.02
$l_{K,Benoit-Doty}$ (nm)	15.8 ± 1.4	10.2 ± 0.8	13.1 ± 1.2
$l_{K\ Koyama}$ (nm)	14.8 ± 1.0	10.5 ± 0.8	12.7 ± 1.9
C_∞	24.7 ± 2.7	20.1 ± 1.6	25.0 ± 3.0

[a] The exponents and amplitude factors were derived from eq 13 with similar relationships for A_2 and $[\eta]$ where ν_g, a_{A_2}, and a_η are the exponents in the molar mass dependencies of R_g and R_h, the second viral coefficient and the intrinsic viscosity, respectively. The theoretical $\nu_{scal,j}$ were derived via scaling relationships $\nu_{scal,R} = (a_{A_2} + 2)/3$ and $\nu_{scal,\eta} = (a_\eta+1)/3$, respectively. Kuhn segment lengths l_K were obtained from the molar mass dependence of R_g according to the Benoit–Doty relationship eq 18a for polydisperse chains with $M_w/M_n = 2$ and from the angular dependence of scattered light using the Koyama theory of wormlike chains. The characteristic ratio was obtained from the approximation $C_\infty = l_K/l$, with the bond length $l = O_1-O_4'$ distance.
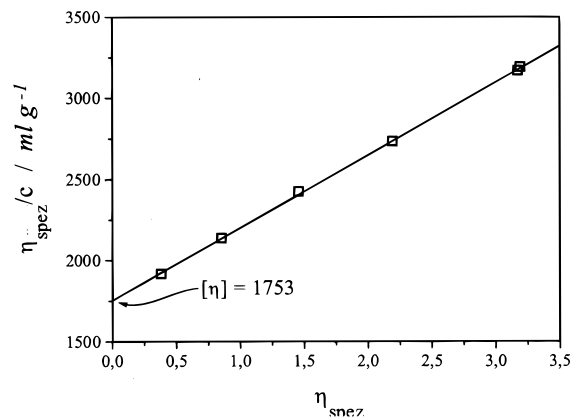

Figure 9. Dependence of the reduced viscosity η_{spec}/c on the specific viscosity η_{spec} which increases with the concentration (Schulz–Blaschke[33] plot). The corresponding plot against concentration gave a strong upturn that is linearized by the Schulz–Blaschke procedure.
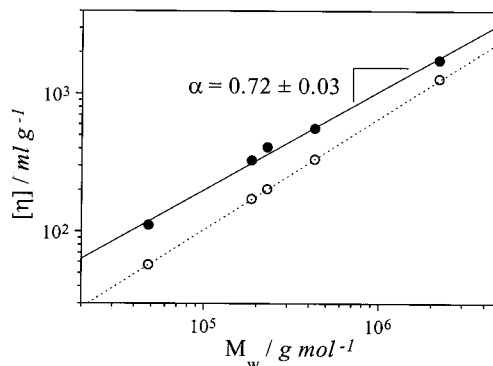
Figure 10. Molar mass dependence of the intrinsic viscosity for cellulose in cuoxam (open circles) and Cd-tren (filled circles).

celluloses and allowed reliable extrapolation to zero concentration. The molar mass dependence of the intrinsic viscosities in Cd-tren and cuoxam is shown in Figure 10. The data are given in Table 4, and the constants and exponents of the power law behavior are listed in Table 5 together with some other molecular
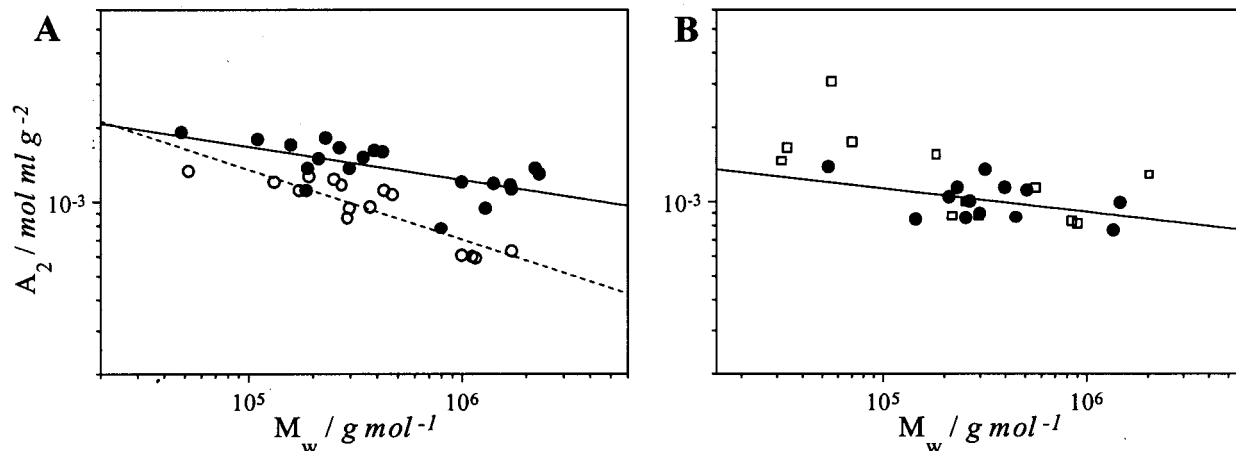
Figure 11. Molar mass dependencies of the second virial coefficients (A) in Cd-tren (filled circles) and Ni-tren (open circles) and (B) in cuoxam (filled circles: this study; open squares: results from ref 8).

parameters. Again common behavior of linear chains is observed.

Second Virial Coefficient. Surprisingly high second virial coefficients were found (Table 4). Figure 11 exhibits the molar mass dependencies in the three cellulose solvents. No differentiation between the three types of cellulose was made. The exponents in the power law dependencies are small, as could be expected for molecularly dispersed linear chains, but vary slightly in value. The reason for this behavior may be found in a certain chain stiffness but could also be seen in marginally good solvent behavior. Mostly the exponents for the various quantities are related to each other. The corresponding scaling relationship for the exponent ν of the radius of gyration and that for the second virial coefficient is given by[34]

$$\nu_g = \frac{a_{A_2} + 2}{3} \tag{15a}$$

and for the viscosity one has

$$\nu_g = \frac{a_\eta + 1}{3} \tag{15b}$$

In Table 5 the experimental ν_{exp} exponents are compared with those obtained via eqs 15a and 15b. The theoretical value of the renormalization group theory (RG) in the good solvent limit is $\nu_{RG} = 0.588$.[35] Larger exponents give evidence for chain stiffness, and smaller ones indicate marginal solution behavior. One notices that the scaling relationships are not well obeyed; in all cases the calculated data for ν are somewhat larger than the directly measured ones. The effect is most developed for cuoxam.

7. Discussion

The present results clearly demonstrate common solution behavior of molecularly dispersed linear chains in the three metal-based solvents Cd-tren, Ni-tren, and cuoxam. Thus, the predictions, made on the basis of crystalline structures of monosaccharides and the study of stability constants of the complexes, are evidently correct and valid.[6,7,11] Cd-tren exhibits the strongest solvating power and could dissolve even the highest degrees of polymerization of bacterial celluloses with $DP_w = 9700$. Ni-tren has lower efficiency and does not dissolve chains of $DP_w > 5500$, and cuoxam seems to

be the weakest solvent. This order corresponds to the values of the ν exponents. However, the order derived from the exponents of the second virial coefficients is different and, and similar ranging is obtained for the intrinsic viscosity. As already mentioned, this could be caused by differences in chain stiffness in these solvents. This effect could be a result of differences in the stability constants for coordinative binding of the metal complexes to the chain. The various effects are considered in detail in the next paragraph.

Chain Stiffness. The rigidity of chains is characterized by two quantities which are the Kuhn segment length l_K and the number of Kuhn segments per contour length N_K. In literature often only the Kuhn segment length is given as stiffness measure, but this can be misleading because the Kuhn length depends on the bond length l between two neighbored repeating units. The bond length of the anhydro glucose unit in cellulose is $l = 0.515$ nm and that for a typical vinyl polymer only $l = 0.25$ nm. Thus, the cellulose stiffness is often overestimated by a factor of 2. More sensible is the use of the dimensionless ratio

$$\frac{l_K}{l} \approx C_\infty \tag{16}$$

which to a good approximation is Flory's characteristic ratio and a measure for rotational hindrance of the units around their bonds.[36]

For sufficiently long chains when $qR_g > 2$, the Kuhn segment length and the number of Kuhn segments can be derived from the angular dependence of the scattered light. In the region of large qR_g values the angular dependence becomes sensitive to the molecular structure. Analysis of the curves becomes possible by application of Koyama's theory[37−39] for wormlike chains. The rigid-rod properties of the Kuhn segment have to be taken into account, which are effective at very large q values. The rod properties are best recognized in the Casassa−Holtzer plot.[40,41] Here the scattering intensity R_θ is multiplied by the magnitude of the q-vector which for long rods gives a constant plateau value that no longer depends on the q value

$$\frac{qR_\theta}{Kc} \to \pi M_L = \pi\left(\frac{M}{L}\right) \tag{17}$$

where M is the molar mass of the rod, L is the length,
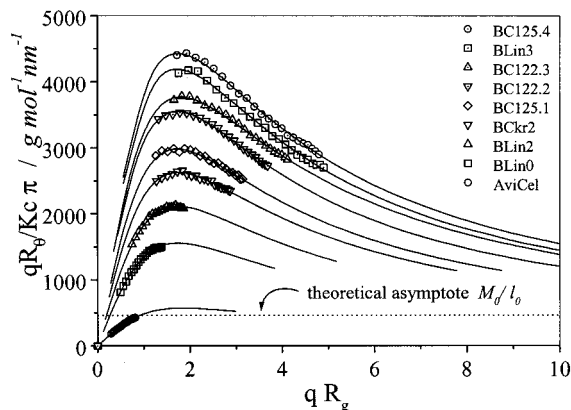
Figure 12. Casassa−Holtzer plots for nine cellulose samples in Cd-tren. The lines correspond to best fits via the Koyama theory[37] of wormlike chains. Similar curves were obtained in the other two solvents.

and M_L is the linear mass density. The latter can be calculated from the molar mass and the bond length of the repeating unit in cellulose which gives $M_L = 314.56$ g/(mol nm). The asymptote is reached from below for rigid rods, but a maximum is passed for semiflexible chains, where the ratio of this maximum height to the plateau value of the rod increases with the number of Kuhn segments and is thus a measure of flexibility.[42] Figure 12 shows such Casassa−Holtzer plots for nine samples measured in Cd-tren. The full lines correspond to fits by the Koyama theory[37] using the above-mentioned linear mass density. The fits were done with a special program[39] that approached the best solution by an iterative process. Physically reasonable constraints had to be set as initial values. Similar curves were obtained with the other solvents. The reliability of the fits was controlled with the radius of gyration. Benoit and Doty[43] derived an equation for the radius of gyration for chains of different stiffness (i.e., Kuhn segment length and number of Kuhn segments). This relationship was complemented by Schmidt,[44] who performed the average for Schulz−Zimm length distributions. We assumed a most probable distribution ($M_w/M_n = 2$) for all samples. The radius of gyration now can be expressed by the simple relationship

$$R_g = L_w \left[\frac{1}{4(1 + N_K)} \right]^{1/2} \quad (18a)$$

where

$$L_w = l\mathrm{DP}_w = l_K N_K \quad (18b)$$

The results of the fits are collected in Table 5. The difference in stiffness is not pronounced; apparently, cellulose has the highest chain stiffness in Cd-tren and the weakest in Ni-tren. This conclusion is now in agreement with order in the exponents a_{A_2} for the second virial coefficient.

Fujita[45] collected data from polymers of very different rigidity and plotted R_g^2/l_K^2 against N_K in a double-logarithmic scale. He also checked the relationships for influences of excluded volume. Figure 13 shows the result for monodisperse chains and for chains with most probable distribution. Fujita noticed that the excluded volume has an effect only when the chain is longer than $50 N_K$. Such an influence should be noticeable for
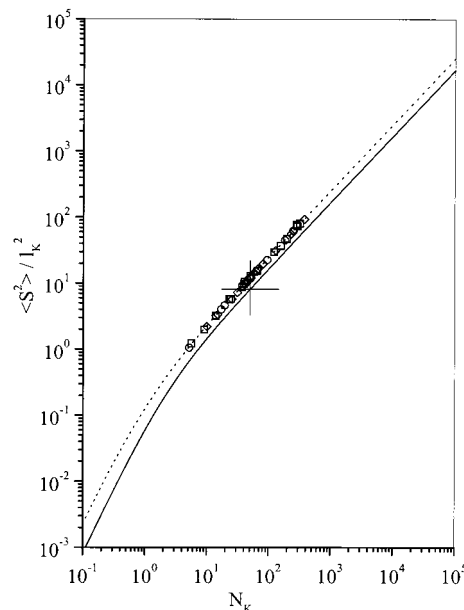

Figure 13. Plot of $(R_g/l_K)^2$ against the number of Kuhn segments N_K per chain according to Fijita.[45] Symbols refer to measurements, full line refers to monodisperse chains, dashed line refers to polydisperse chains with $M_w/M_n = 2$. In good solvents the effect of excluded volume becomes noticeable when $N_K > 50$, indicated by the cross. The assumption of polydisperse cellulose chains is well confirmed with the present samples. l_K is the Kuhn segment length, and $\langle S^2 \rangle = R_g^2$ is the mean-square radius of gyration.
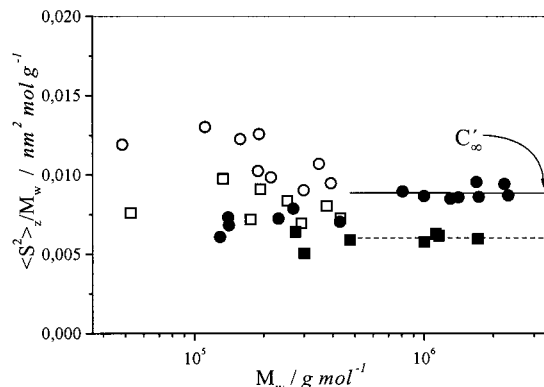
Figure 14. Plot of $\langle S^2 \rangle / M_w$ against the molar mass M_w (A) for cellulose in Cd-tren (circles) and Ni-tren (squares) (B) in cuoxam (circles: this study, squares: ref 8, see text). The filled symbols refer to native and the open to pulp celluloses. No influence of intrachain excluded-volume interaction is recognized. $C_\infty' = (l^2/6M_0)C_\infty$.

samples with $DP_w > 1600$. Our data follow the relationship for polydisperse chains without excluded-volume effects.

A more sensitive check can be made by considering the ratio R_g^2/M_w. A constant plateau should be reached for chains that approach the behavior of Gaussian chains, whereas in typical good solvents the plot should approach an increase with power of 0.176.[35,46] In all three solvents a Gaussian plateau is reached (Figure 14) which indicates that the systems are not yet in the region of thermodynamically good solvents. The plateau height is proportional to Flory's characteristic ratio at large chain lengths. Apparently Ni-tren is less strongly bound to the cellulose chain than Cd-tren, which is equivalent to lower chain stiffness in Ni-tren than in Cd-tren.
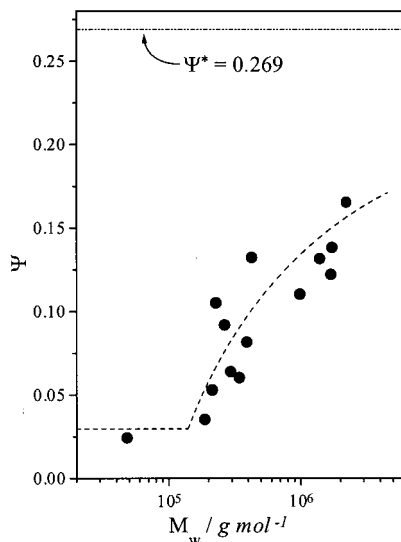
Figure 15. Coil interpenetration function $\Psi(z)$ as a function of the molar mass for cellulose in the three metal-based solvents: (A) Cd-tren, (B) Ni-tren, (C) cuoxam. According to Fujita,[42] the effect of excluded volume becomes not effective before $N_K = 50$. The asymptotic limit of $\Psi^* = 0.269$ is not reached, because N_K remained too small even for the longest cellulose chains.

A special comment is required concerning the behavior of cuoxam. With freshly prepared samples again a plateau of almost the same height as for Ni-tren is obtained. In previous papers[8,9] a different behavior was reported according to which the values pass through a maximum, which is larger than the plateau height, and then decreased strongly. As already mentioned, this difference in behavior may be an effect of aging. In our interpretation colloid clusters of the solvent are adsorbed onto the chain. Part of the chains with adsorbed clusters are removed on ultracentrifugation. Now an apparent molar mass is measured that is smaller by the reduced concentration. Adsorption of a colloid cluster can also cause stiffening of the chain. The downturn beyond the maximum was interpreted as intramolecular cross-linking. This view remains valid, but the intramolecular reaction would be caused here not by a single complex but more likely due to coupling via a colloid cluster.

Interpenetration Function Ψ. The second virial coefficient is described in general terms by the equation[46]

$$A_2 = 4\pi^{3/2} N_a \frac{R_g^{\,3}}{M_w^{\,2}} \Psi(z) \qquad (19)$$

with z an interaction parameter given by[46]

$$z = \left(\frac{3}{2\pi l_K^{\,2}}\right)^{3/2} \beta N_K^{\,1/2} \qquad (20)$$

in which β is the binary cluster integral that describes the excluded volume of a Kuhn segment. The function $\Psi(z)$ describes how deep two coils of macromolecules can penetrate each other. Under Θ-conditions one has $z = 0$ and full interpenetration, i.e., $\Psi(z) = 0$. With increasing repulsive interactions z and $\Psi(z)$ increase until a constant value $\Psi^* = 0.269$ is reached.[35] (Note that z increases proportional to $N_K^{1/2}$.) Figure 15 shows a plot

of $\Psi(z)$ as a function of $M_w^{1/2}$. The curves start at very low values, and only beyond $M_w > 150\,000$ (DP$_w$ > 900, N_K > 35) does a sharp increase occur. This confirms Fujita's findings that excluded-volume effects become noticeable only for $N_K > 50$. Thus, the cellulose chains exist in the present solvents in a transition region from marginal to good-solvent behavior, not because of a weak solvation power, but because of the existing chain stiffness and small number of Kuhn segments. In this transition regime scaling relationships are not exactly fulfilled.

Another point is of interest. Because of the chain stiffness the second virial coefficient at low molar mass approaches that of a chain of less than one Kuhn segment in length. If the Kuhn segement is approximately assumed being a rigid cylinder, we can use Zimm's equation for the second virial coefficient[46,47] which is given by

$$A_2 = \pi N_a d_{cross} \frac{l_K^{\,2}}{(2M_{l_K})^2} \qquad (21)$$

which allows us to estimate the cross-sectional diameter d_{cross} of the cylinder. Taking the extrapolated values of A_2 at $M_{l_K} = 2400$, 1700, and 2060 for Cd-tren, Ni-tren, and cuoxam, respectively, one obtains cross-sectional diameter $d_{cross} = 0.54$, 0.36, and 0.52 nm and for the axial ratios $p = l_K/d_{cross} = 27$, 30, and 25, respectively. On average the diameters are $\langle d_{cross} \rangle = 0.48 \pm 0.12$ nm and an axial ratio of $\langle p \rangle = 27 \pm 7$ with an estimated error of 25%. The data are, of course, rough estimations but well in the range of expectation.

The $\rho = R_g/R_h$ Parameter. The last quantity to be discussed is the $\rho = R_g/R_h$ parameter which also gives some indications for the structure of objects in solution.[30,48,49] The properties result from the fact that the radius of gyration is solely geometrically defined, but the hydrodynamic radius in addition is determined by hydrodynamics interaction among the segments in a coil. Translational diffusion of a macromolecule can often be described by an equivalent sphere that partially can be drained by the solvent.[46,50,51] For a high segment density, the draining is weak and the hydrodynamic interaction becomes large. For wormlike chains, on the other hand, the solvent can deeply penetrate into the rather open coil, and the sphere radius is small. For impenetrable spheres with a well-defined surface the ρ parameter has a value of $\rho = 0.778$. It becomes larger for branched macromolecules ($\rho \approx 1.0$ in the limit of many branching units per macromolecule[30]), increases further for flexible linear chains ($\rho = 1.23-1.5$), and assumes values larger than $\rho = 2$ for long cylinders.[31] Polydispersity and excluded-volume effects increase the value further.[30,31,52] The hydrodynamic radius R_h depends only weakly on these quantities, but the radius of gyration is rather sensitive to polydispersity. Within the scatter of experimental accuracy there was no dependence of the ρ parameter on the molar mass. The values in the three solvents are as follows: Cd-tren, $\rho = 1.82 \pm 0.14$; Ni-tren, $\rho = 2.50 \pm 0.19$; and cuoxam, $\rho = 2.51 \pm 0.24$. Accordingly, Cd-tren behaves like a polydisperse Gaussian coil with only weak indications for chain stiffness. From the values for the two other solvents a stronger influence of chain stiffness seemed to be effective. This result is at variance with the actually determined chain stiffness. This leads to the

conclusion that the coordinatively bound metal complex may have a special contribution to the hydrodynamic interaction that so far is not known to us.

8. Conclusions

Cellulose can be dissolved to a molecular level in aqueous metal-based solvents. Most effective is a coordinative binding of the metal complex to the deprotonated olate anions in the C2 and C3 position of the anhydro glucose units in the chain. Apparently, coordinative binding occurs on every AGU. The three solvents cuoxam, Ni-tren, and Cd-tren do not differ much in behavior and show good solvent behavior for cellulose. However, the well-known asymptotes for flexible lineare chains were not yet reached. The reason for this may be found in chain stiffness that is about 7−12 times larger than for polystyrene. The number of Kuhn segment lengths per chain exceeded only in a few cases the limit of $N_K > 50$ (indicated by a cross in Figure 12). At this point, according to Fujita,[45] the influence of excluded volume becomes noticeable. This statement is confirmed by the coil interpenetration function $\Psi(z)$ that just at this point started to increase but remained still much smaller than the asymptotic value of 0.269. Much longer cellulose chains are required before the asymptote can be reached. The chain stiffness is very likely caused by an enhanced strength of the hydrogen bonds between the deprotonated olate O_3^- and the ring oxygen of the next AGU.[11] In cellulose successive anhydro glucose units are rotated by 180°. Thus, the chain resembles a conformational alternating copolymer with cellobiose as a repeating unit. Thus, the hydrogen-bonding system reduces segmental mobility in a similar manner as in ladder polymers.

Appendix: Notation and Abbreviations

Throughout this paper notations and abbreviations are used which are not common in polymer science. A short explanation is listed here.

Alcohols are commonly denoted by endings of *-ol*; the corresponding deprotonated alcohol is denoted as *olate.* Example: methanol and methanolate, respectively. If two OH groups are deprotonated, the compound is called *diolate.*

In a short-hand writing the organic ligands are abbrevated as en = ethylenediamine and -tren = tris-(2-aminoethyleneamine) = $N(CH_2-CH_2-NH_2)_3$. Ethylenediamine is a bidentate and tris(2-aminoethylene amine) a tetradentate ligand (compare Figures 1 and 2).

Complexes are called *homoleptic* when all ligands in a complex are the same in composition. Complexes with different kinds of ligands are denoted as *heteroleptic.*

References and Notes

(1) (a) Staudinger, H. *Die hochmolekularen organischen Verbindungen−Kautschuk und Cellulose*; Springer: Berlin 1932. (b) *Arbeitserinnerungen*; Hütig: Heidelberg, 1961 (English translation: *From Organic Chemistry to Macromolecules*; Wiley: New York, 1970).
(2) Staudinger, H. Fritschi, J. *Helv. Chim. Acta* **1922**, *5*, 785.
(3) Fengel, D.; Wegener, G. *Wood*; de Gruyter: Berlin 1989.
(4) (a) Schulz, L.; Burchard, W.; Dönges, R. In Heinze, T. J., Glasser, W. G., Eds.; *Cellulose Derivatives, Modifications Characterization and Nanostructures*; ASC Symp. Ser. **1998**, *688*, 218. (b) Schulz, L.; Seger, B.; Burchard, W. *Macromol. Chem. Phys.,* in press.
(5) Schweizer, E. J. *J. Prakt. Chem.* **1857**, *72*, 109.
(6) Fuchs, R.; Habermann, N.; Klüfers, P. *Angew. Chem., Int. Ed. Engl.* **1993**, *32*, 852.
(7) Burchard, W.; Habermann, N.; Klüfers, P.; Seger, B.; Wilhelm, U. *Angew. Chem., Int. Ed. Engl.* **1994**, *33*, 884.
(8) Burchard, W.; Seger, B. *Macromol. Symp.* **1994**, *83*, 291.
(9) Seger, B.; Aberle, T.; Burchard, W. *Carbohydr. Polym.* **1996**, *31*, 105.
(10) (a) Jayme, G. *Tappi* **1962**, *44*, 299. (b) New Solvents. In *Cellulose and Cellulose Derivatives*; Bikales, N. M., Segal, L., Eds.; Wiley: New York, 1971; pp 381−410.
(11) (a) Burger, J.; Kettenbach, G.; Klüfers, P. *Macromol. Symp.* **1995**, *99*, 113. (b) Kettenbach, G.; Klüfers, P.; Mayer, P. *Macromol. Symp.* **1997**, *120*, 291.
(12) (a) Gardner, K. H.; Blackwell, J. *Biopolymers* **1974**, *13*, 1975. (b) Kolpak, P. J.; Blackwell, J. *Macromolecules* **1976**, *9*, 273.
(13) Normann, W. *Chem. Ztg.* **1906**, *30*, 584.
(14) Klaassen, M.; Klüfers, P. *Z. Anorg. Allg. Chem.* **1993**, *619*, 661.
(15) Traube, W. *Ber. Dtsch. Chem. Ges.* **1921**, *54*, 3320.
(16) Ballauff, M.; Kettenbach, G.; Hanemann, O.; Klüfers, P. *Chem. Eur. J.*, in press.
(17) Ballauff, M.; Hanemann, O. *Macromolecules* **1997**, *30*, 7638.
(18) Huglin, M. B. *Light Scattering from Polymer Solutions*; Academic Press: London, 1972; Chapter 6, pp 165−331.
(19) Strazielle, C. *Light scattering in mixed solvents.* In Huglin, M. B., Ed.; *Light Scattering from Polymer Solutions;* Academic Press: London, 1972.
(20) Compare also: Kirkwood, J. G.; Goldberg, R. J. *J. Chem. Phys.* **1950**, *18*, 54. Stockmayer, W. H. *J. Chem. Phys.* **1950**, *18*, 58.
(21) Gralén, N. Ph.D. Thesis, University of Uppsala, 1944.
(22) Burchard, W.; Husemann, E. *Makromol. Chem.* **1961**, *44−46*, 358.
(23) Dandliker, W. B.; Kraut, J. *J. Am. Chem. Soc.* **1956**, *78*, 2380.
(24) Williams, G.; Watts, O. C. *Some aspects of dielectric relaxation of amorpheous polymers.* In Diehl, P., Fluck, E., Kosfeld, R., Eds.; *NMR: Basis Principles and Progress*; Springer: Berlin 1971; Vol. 4, p 271.
(25) Berne, B. J.; Pecora, R. *Dynamic Light Scattering*; Wiley: New York, 1976.
(26) Brown, W., Ed. *Dynamic Light Scattering: Methods and Some Applications*; Clarendon Press: Oxford, 1993.
(27) Brown, W., Ed.; *Light Scattering: Principles and Development*; Clarendon Press: Oxford 1996.
(28) Klemm, D.; Dugarmaa, S. Manuscript in preparation.
(29) Bantle, S.; Schmidt, M.; Burchard, W. *Macromolecules* **1982**, *15*, 1604.
(30) Burchard, W.; Schmidt, M.; Stockmayer, W. H. *Macromolecules* **1980**, *13*, 1265.
(31) Schmidt, M.; Stockmayer, W. H. *Macromolecules* **1984**, *17*, 509.
(32) Seger, B. Ph.D. Thesis, University of Freiburg, 1996.
(33) Schulz, G. V.; Blaschke, F. *J. Prakt. Chem.* **1941**, *148*, 136.
(34) De Gennes, P.-G. *Scaling Concepts in Polymer Physics*; Cornell University Press: Ithaca, NY, 1979.
(35) Freed, K. F. *Renormalization Theory of Macromolecules*; Wiley: New York, 1987.
(36) Flory, P. J. *Statistical Mechanics of Chain Molecules*; Wiley: New York, 1969.
(37) Koyama, R. *J. Phys. Soc. Jpn.* **1973**, *34*, 1029.
(38) Denkinger, P.; Burchard, W. *J. Polym. Sci., Polym. Phys.* **1991**, *B29*, 539.
(39) Dolega, R. *Special Development of Laboratory Burchard*, University of Freiburg, 1990.
(40) Casassa, E. F. *J. Chem. Phys.* **1955**, *23*, 596.
(41) Holtzer, A. *J. Polym. Sci.* **1955**, *17*, 432.
(42) Schmidt, M.; Paradossi, G.; Burchard, W. *Makromol. Chem., Rapid Commun.* **1985**, *6*, 767.
(43) Benoit, H.; Doty, P. *J. Phys. Chem.* **1953**, *57*, 958.
(44) Schmidt, M. *Macromolecules* **1984**, *17*, 553.
(45) Fujita, H. *Macromolecules* **1988**, *21*, 129.
(46) Yamakawa, H. *Modern Theory of Polymer Solutions*; Harper & Row: New York, 1971.
(47) Zimm, B. H. *J. Chem. Phys.* **1948**, *16*, 1099.

(48) The reciprocal parameter $\zeta = 1/\rho = R_h/R_g$ was introduced for a linear chain by Tanford (ref 45) and is used occasionally also for the characterization of other architectures.

(49) Tanford, C. *Physical Chemistry of Macromolecules*; Wiley: New York, 1967; p 344.

(50) Kirkwood, J. G.; Riseman, J. *J. Phys. Chem.* **1948**, *16*, 565.

(51) Debye, P.; Bueche, A. M. *J. Chem. Phys.* **1948**, *16*, 573.

(52) Burchard, W. *Combined Static and Dynamic Light Scattering.* In Brown, W., Ed.; *Light Scattering: Principles and Some Applications*; Clarendon Press: Oxford, 1996.